Full-Wave Spectral-Domain Analysis of Coplanar Strips

Sotirios G. Pintzos, *Member, IEEE*

Abstract—**In this paper a dynamic analysis of coplanar strips (CPS's) is presented. A spectral-domain stationary expression for the propagation constant has been derived making use of proven concepts of electromagnetic theory (e.g. the "reaction concept"). For the strip surface current distribution, which is the trial quantity in the stationary expression, a suitable approximation is used. The numerical results, obtained in a straightforward and efficient way, are in excellent agreement with results arrived at by means of more complex methods. Further, the characteristic impedance of CPS's has been determined on the base of two commonly used definitions. The numerical results show a novel aspect of the dynamic behavior of the impedance (power-related definition) in the upper frequency region.**

I. Introduction

COPLANAR strips (CPS's) make up an open planar wave-guiding structure which along with its complementary configuration, the coplanar waveguide (CPW), constitutes the "family" of what are called coplanar lines. CPS's comprise two parallel metallic strips generally of equal width placed on the same (upper) side of an ungrounded dielectric slab (Fig. 1). The possibility of easy mounting of both shunted elements and elements in series and the relatively large range of practically realizable impedance values, as well as the availability of a magnetic field configuration of elliptical polarization, which is necessary for the realization of nonreciprocal propagation behavior, may be mentioned as some important features of this transmission line. However, so far CPS's have found only moderate application as basic transmission lines for the implementation of microwave components. The strips have mainly been used in combination with the established planar lines, microstrip and microslotline, in the context of specific hybrid and (recently) monolithic MIC applications.

Wen introduced coplanar strips 1969 in a paper [2] in which the new line was investigated by means of a quasi-static method and under the assumption of infinite extent of the dielectric substrate. Knorr *et al.* were the first to publish a full-wave analysis of CPS's using Galerkin's method in the Fourier transform domain [1]. A limited number of publications have been presented on the basis of the quasi-static approach [9]–[11].

The purpose of this paper is to present new results on the dynamic (dispersive) behavior of the line's propagation characteristics, in particular the characteristic impedance, and to demonstrate the generality and ease of application of the present method as well as its efficiency and reliability.

Manuscript received November 30, 1989; revised August 7, 1990.

The author is with the Research Center of the Hellenic Navy (GETEN), MOD, Cholargos, Athens, Greece.

IEEE Log Number 9041084.

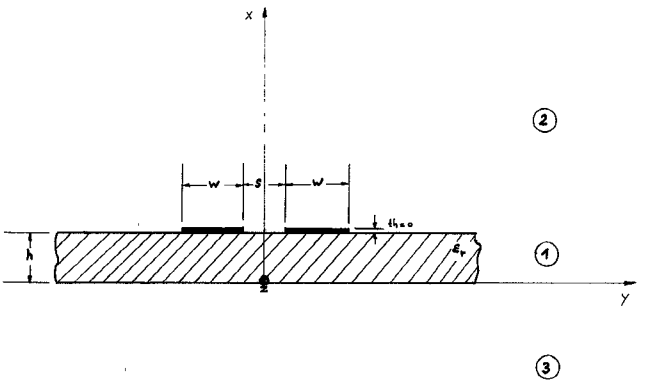

Fig. 1. Cross section of coplanar strips.

By means of a proven procedure [3], [6] a spectral-domain variational expression for the propagation constant has been formulated and numerical results for the dominant propagation mode of CPS's have been obtained. They compare favorably with corresponding results in previous publications [1]. Further, the characteristic impedance has been calculated on the basis of two commonly used definitions—"ereff" and "transported power." It should be noted here that the numerical results arrived at using the more general, transported power definition show an impedance behavior which is characterized by a monotonic decrease up to a certain frequency range and a clear upward trend toward the upper frequency region. This finding constitutes a novel aspect of the dynamic behavior of CPS's given the fact that published results up to this date seem to anticipate a steady decrease of the characteristic impedance with increasing frequency [1].

II. Variational Method

Fig. 1 shows the physical construction of CPS's. The strips are assumed to be without losses and the dielectric substrate is characterized by the dielectric constant, which is taken as an isotropic scalar quantity. Further, the strips are assumed to be of negligible thickness. In our case, for the determination of the propagation constant, a variational method is used in connection with what is referred to as the reaction concept [5], [4]. Before proceeding to apply this concept to the structure under investigation, an equivalent, simpler model will be presented. In compliance with the equivalence theorem, the metal strips are schematically replaced by "magnetic wall" (flat tube shaped) coverings outside of which electric and magnetic Huygens's sources are introduced. The

interior of these coverings being field-free, the equivalent electric and magnetic source currents are given by $\vec{J} = \vec{n} \times \vec{H}$ and $\vec{M} = \vec{E} \times \vec{n}$, respectively, $\vec{n}$ being the unit vector normal to the fictitious enclosure. However in such a configuration, the magnetic source $\vec{M}$, owing to its proximity to the magnetic wall, is neutralized ("short-circuited"). Therefore with respect to the described model and referring to the definition of "reaction," an interaction is taking place only between the electric field and the associated electric current source, $\vec{J} = \vec{J}_s \cdot \delta(x - h)$:

$$\mathrm{SR} = \int_V \vec{E} \cdot \vec{J}\, dV. \tag{1}$$

This expression represents the "self-reaction" (SR) of the field on its own (fictitious) source.

On the other side, the field supported by the configuration under investigation is source-free; therefore its true self-reaction must vanish. It can be demonstrated that by requiring an approximate expression for the self-reaction to be equal to the correct one, a stationary formula for the quantity of interest (propagation constant) can be obtained [4]. The rationale of our approach is then to derive such a variational formula by first formulating, via the simple equivalent model and on the basis of (1), an approximate expression for the self-reaction and then to equate this expression to the exact one, which, as has been shown before, is zero. A stationary formula for the propagation constant is then obtained in the form of the following implicit characteristic equation:

$$\int_{-\infty}^{\infty} \vec{E} \cdot \vec{J}_s\, dy = 0. \tag{2}$$

In our case, the surface current density $\vec{J}_s$ on the strips is the trial quantity for which reasonable approximations can be made. Its distribution can be thought of as a dynamic extrapolation of the (known) static charge or stationary current distribution on two metallic strips in a homogeneous medium. This assumption is legitimized by the fact that the dominant mode of CPS's is basically of quasi-TEM nature.

Equation (2) is now the starting point for the following analysis procedure. For the final formulation of this stationary expression for evaluation purposes, the electric field, $\vec{E}$, must be given in terms of the assumed current distribution. Its determination via the field equations will be presented in the following.

III. Field Determination and Stationary Expression

The propagation modes which can be supported by an inhomogeneous, cylindrical structure such as that formed by CPS's are of hybrid type, having both an electrical and magnetic component in the z direction. Thus, the field components implied in (2) have to be derived from two vector potentials in the longitudinal (Cartesian) direction, $\vec{A} = \vec{u}_z \Psi^E$ and $\vec{F} = \vec{u}_z \Psi^H$ [4], the superscripts E and H denoting electric and magnetic, respectively.

The solution of Helmholtz's equation for $\Psi^{E,H}$ can formally be cast in the form

$$\Psi^{E,H}(x, y, z) = \Psi^{E,H}(x, y) \cdot e^{-j\beta z}. \tag{3}$$

Because of the infinite extent of the CPS's (Fig. 1) and the homogeneity (for $x = \text{const}$) in the y direction, (3) is appropriately given in form of a Fourier integral:

$$\Psi^{E,H}(x, y, z) = \int_{-\infty}^{\infty} \overline{\Psi}^{E,H}(x, k_y) \cdot e^{jk_y y}\, dk_y \cdot e^{-j\beta z} \tag{4}$$

where $\overline{\Psi}^{E,H}(x, k_y)$ is the Fourier transform of $\Psi^{E,H}(x, y)$ with respect to y. By means of (4) Helmholtz's equation is reduced to an ordinary differential equation in one variable:

$$\frac{d^2 \overline{\Psi}^{E,H}(x, k_y)}{dx^2} + \gamma_i^2 \overline{\Psi}^{E,H}(x, k_y) = 0 \tag{5}$$

where

$$\gamma_i^2 = k_y^2 + \beta^2 - \epsilon_{ri} k_0^2 \tag{6}$$

$i = 1,2,3$ designating the subregions in Fig. 1 and k_0 being the wavenumber in vacuum. Thus the x dependence of the field has to be described by harmonic functions. The quantity $\Psi^{E,H}(x, y)$ is then specified for the particular subregions as follows.

Region 1:

$$\Psi^{E,H}(x, y) = \int_{-\infty}^{\infty} \left[A_1^{E,H}(k) \cdot \cosh(\gamma_1 x) + B_1^{E,H}(k_y) \sinh(\gamma_1 x) \right] e^{jk_y y}\, dk_y \tag{7a}$$

$$\gamma_1^2 + k_0^2 \epsilon_r = k_y^2 + \beta^2. \tag{7b}$$

Region 2:

$$\Psi^{E,H}(x, y) = \int_{-\infty}^{\infty} A_2^{E,H}(k_y) \cdot e^{-\gamma_2 (x-h)} \cdot e^{jk_y y}\, dk_y \tag{7c}$$

$$\gamma_2^2 + k_0^2 = k_y^2 + \beta^2. \tag{7d}$$

Region 3:

$$\Psi^{E,H}(x, y) = \int_{-\infty}^{\infty} A_3^{E,H}(k_y) \cdot e^{\gamma_3 x} \cdot e^{jk_y y}\, dk_y \tag{7e}$$

$$\gamma_3^2 + k_0^2 = k_y^2 + \beta^2 \qquad (\gamma_3 = \gamma_2). \tag{7f}$$

The next step is to determine the field components needed for the formulation of the continuity conditions valid at $x = 0$ and $x = h$. For $x = h$,

$$E_{y1} = E_{y2} \tag{8a}$$

$$E_{z1} = E_{z2} \tag{8b}$$

$$H_{y1} - H_{y2} = -J_{sz} \tag{8c}$$

$$H_{z1} - H_{z2} = J_{sy}. \tag{8d}$$

For $x = 0$,

$$E_{y1} = E_{y3} \tag{9a}$$

$$E_{z1} = E_{z3} \tag{9b}$$

$$H_{y1} = H_{y3} \tag{9c}$$

$$H_{z1} = H_{z3}. \tag{9d}$$

J_{sy} and J_{sz} are the transversal and longitudinal components respectively of the surface current density on the strips. They can also, like the field components, be given in the form of Fourier integrals in terms of their respective transforms ($\bar{J}_{sy}$ and $\bar{J}_{sz}$).

Inserting the implied field and current components into (8) and (9), a system of eight linear equations for the eight

unknown spectral amplitude coefficients, $A_1^{E,H}$, $B_1^{E,H}$, $A_2^{E,H}$, and $A_3^{E,H}$, is eventually obtained (Appendix I). By determining these coefficients, the transformed field components can be expressed in terms of the Fourier transform of the current distribution on the strips.

With respect to this distribution the assumption is made at this point that the transversal current component is negligible compared with the longitudinal component. Equation (2) can then be simply written as

$$\int_{-\infty}^{\infty} E_z(x=h)\cdot J_{sz}\cdot dy = 0. \tag{10}$$

Incorporating E_z (as a Fourier integral) into (10) and interchanging the integration sequence between k_y and y, the stationary expression assumes the form (Parseval's theorem)

$$\int_{-\infty}^{\infty} \bar{E}_z(x=h,k_y)\cdot \bar{J}_{sz}(-k_y)\cdot dk_y = 0. \tag{11}$$

The formulation of $\bar{E}_z(k_y)$ in terms of $\bar{J}_{sz}(k_y)$ and appropriate algebraic manipulations lead to the final form of the stationary expression:

$$\int_0^{\infty} \frac{(\epsilon_r-\epsilon_{r\,\mathrm{eff}})\cdot\{e^{-1}\cdot\gamma_1^{-1}\cdot\gamma_2\cdot\tanh(\gamma_1\cdot h)\cdot E_1\cdot E_2^{-1}\cdot[\tanh(\gamma_1\cdot h)\cdot\gamma_1+\epsilon_1\cdot\gamma_2]+[\gamma_1\cdot\tanh(\gamma_1\cdot h)+\epsilon_2\cdot\gamma_2]\}\cdot|\bar{J}_{sz}(k_y)|^2\cdot dk_y}{E_3\cdot\{[\gamma_1\cdot\tanh(\gamma_1\cdot h)+\epsilon_2\cdot\gamma_2]\cdot[\gamma_1\cdot\tanh(\gamma_1\cdot h)+\epsilon_3\cdot\gamma_2]+e^{-2}\cdot(\epsilon_r^{-1}-1)\cdot\gamma_2^2\cdot\gamma_1^{-1}\cdot\tanh(\gamma_1\cdot h)\cdot\epsilon_4\cdot[\gamma_1\tanh(\gamma_1\cdot h)+\epsilon_1\cdot\gamma_2]\}} = 0. \tag{12}$$

The integration limits have been changed (0 to ∞) because the integrand is an even function of k_y. Further, it may be noticed that in place of the propagation constant β, the equivalent quantity $\epsilon_{r\,\mathrm{eff}}$(ereff) has been introduced, defined as $\epsilon_{r\,\mathrm{eff}} = (\beta/k_0)^2$. Expressions for E_1, E_2, E_3, ϵ_1, ϵ_2, ϵ_3, ϵ_4, and e are given in Appendixes I and II. Thus a simple variational formula has been derived through which the dispersion characteristic of CPS's can be determined in a straightforward and numerically economic way. These aspects should be appropriately appreciated concerning CAD applications. The numerical treatment of (12) as well as representative results will be presented later.

IV. Characteristic Impedance

The characteristic impedance of CPS has been determined on the basis of two different definitions commonly used for MIC transmission lines. The first is associated with the static characteristic impedance of the corresponding homogeneous structure, which in our case is represented by two metallic strips embedded in a homogeneous medium. The dynamic aspect is taken into account by schematically replacing the relative permeability of the homogeneous medium with the effective dielectric constant of the (inhomogeneous) structure under investigation ("ereff" definition):

$$Z_c = \frac{Z_{c0}}{\sqrt{\epsilon_{r\,\mathrm{eff}}}} \tag{13}$$

where Z_{c0} is the static characteristic impedance of the homogeneous structure in vacuum, for which the following exact formula is valid:

$$Z_{c0} = \eta\frac{K(k)}{K(k')}. \tag{14}$$

Here η is the free-space wave impedance, and $K(k)$ and $K(k')$ are the complete elliptic integrals of the first kind. The module k and its complementary module k' are geometrically related parameters (Fig. 1):

$$k = \frac{s}{s+2\cdot w} \qquad k' = \sqrt{1-k^2}.$$

Given the fact that there is always a monotonic increase in the effective dielectric constant with increasing frequency, the characteristic impedance based on this definition will consequently decrease with increasing frequency.

According to the second, more general, and now established definition, the characteristic impedance is formulated as

$$Z_c = \frac{P}{|I_z|^2} \tag{15}$$

where P is the real power transported along the line and I_z is the current on one strip.

In order to determine the transported power P, the integration of the longitudinal component of the Poynting vector over the infinite cross section of the line is necessary:

$$P = \mathrm{Re}\int_{-\infty}^{\infty}\int_{-\infty}^{\infty} S_z\cdot dx\,dy$$

$$= \mathrm{Re}\int_{-\infty}^{\infty}\int_{-\infty}^{\infty}\{(E_xH_y^* - E_yH_x^*)\,dy\}\,dx. \tag{16}$$

Making use of Parseval's theorem and the possibility of interchanging the sequence of integrations with respect to k_y and x, we arrive at the following expression for the calculation of the transported power:

$$P = \mathrm{Re}\int_{-\infty}^{\infty}\int_{-\infty}^{\infty}\{(\bar{E}_x(x,k_y)\bar{H}_y^*(x,k_y) - \bar{E}_y(x,k_y)\bar{H}_x^*(x,k_y)\,dx\}\,dk_y. \tag{17}$$

The integration with respect to the spatial variable x can be carried out analytically for each subregion separately given the fact that the x dependences of the field components involved are described by harmonic functions. The results of this integration are obtained in a straightforward manner, but being rather lengthy are not presented here. Now, for the complete evaluation of (17) the remaining integration in the spectral domain is performed by the same numerical means used for evaluating the integral in (12). Further, the strip current in (15) can be formulated as the integral of the current density over the cross section. A current being present only at $x = h$ and suppressing the z dependence, this integral becomes

$$I_z = \int_{-\infty}^{\infty} J_{sz}(y)\,dy. \tag{18}$$

This can be interpreted as the Fourier transform of the surface current density distribution taken at the discrete spectral point $k_y = 0$. The fact that $\bar{J}_{sz}(k_y)$ has to be in any case available for the evaluation of (12) and (17) obviously facilitates the evaluation of the strip current itself and therefore the calculation of Z_c.

Numerical results for the characteristic impedance and a discussion thereof will be presented in the following section.

V. Numerical Results

As can be seen from the formulas pertaining to the characteristic quantities of CPS's, their determination is linked to the availability of the Fourier transform $\bar{J}_{sz}(k_y)$ of the assumed strip current distribution. It has been pointed out that the static charge or stationary current distribution on two metallic strips in a homogeneous dielectric provides an adequate approximation for the current distribution on CPS's. According to [8], the exact current distribution on two metallic strips in vacuum is given by

$$I(y) = \frac{\operatorname{sgn}(y)}{\sqrt{\left[1-\left(\frac{2\cdot y}{s+2\cdot w}\right)^2\right]\left[\left(\frac{2\cdot y}{s+2\cdot w}\right)^2-\left(\frac{s}{s+2\cdot w}\right)^2\right]}}. \tag{19}$$

However, the Fourier transform of such a formula being not available in closed form, a numerical integration is necessary for its calculation. The fact that this (spatial-domain) integration must be performed at all discrete spectral points prescribed by the numerical integration procedure to be applied for the evaluation of the integrals in (12) and (17) would significantly add to the overall computational effort.

It can be argued that another feasible approximation for the distribution of the surface current on (each strip of) CPS's is the static charge distribution on a single (isolated) strip in vacuum, which is exactly known. In this case the CPS current distribution is to be described as

$$J_{sz} = \begin{cases} \dfrac{(\pm 1)\cdot(2/w)}{\sqrt{1-\left(\dfrac{2\cdot y}{w}\pm\dfrac{s+w}{w}\right)^2}} & \text{for } s/2<|x|<s/(s+w) \\ 0 & \text{otherwise.} \end{cases} \tag{20}$$

The same approximation has been used for a first-order solution in [1]. The Fourier transform of (20) is easily obtained, starting with the transform of an isolated strip and applying in the following the shift theorem:

$$\bar{J}_{sz}(k_y) = 0.5j\cdot J_0\left(\frac{k_y\cdot w}{2}\right)\sin\left[k_y\left(\frac{s+w}{2}\right)\right]. \tag{21}$$

J_0 is the Bessel function of the first kind of zero order. The numerical results both for $\epsilon_{r\,\mathrm{eff}}$ and the characteristic impedance presented in this paper are based on (20).

Now, for the numerical treatment of (12), well-known methods are used. For the solution of this implicit equation the "regula falsi" method has proved to be an adequate root determination procedure. The integration of the improper stationary integral is accomplished by means of a Gauss quadrature algorithm. The asymptotic behavior of the integrand is found to be proportional to $|\bar{J}_{sz}(k_y)|^2/k_y$. In cases where $\bar{J}_{sz}(k_y)$ is described by (21) the integrand becomes $\sim k_y^{-2}$. This fact allows for setting of the upper integration limit at convenient values. For example, a typical value of 250 [1/cm] for the upper integration limit $k_{y\infty}$ is considered sufficient for configuration parameter sets similar to those used in this paper.

Numerical results for the propagation constant or, equivalently, for the effective relative dielectric constant (ereff)

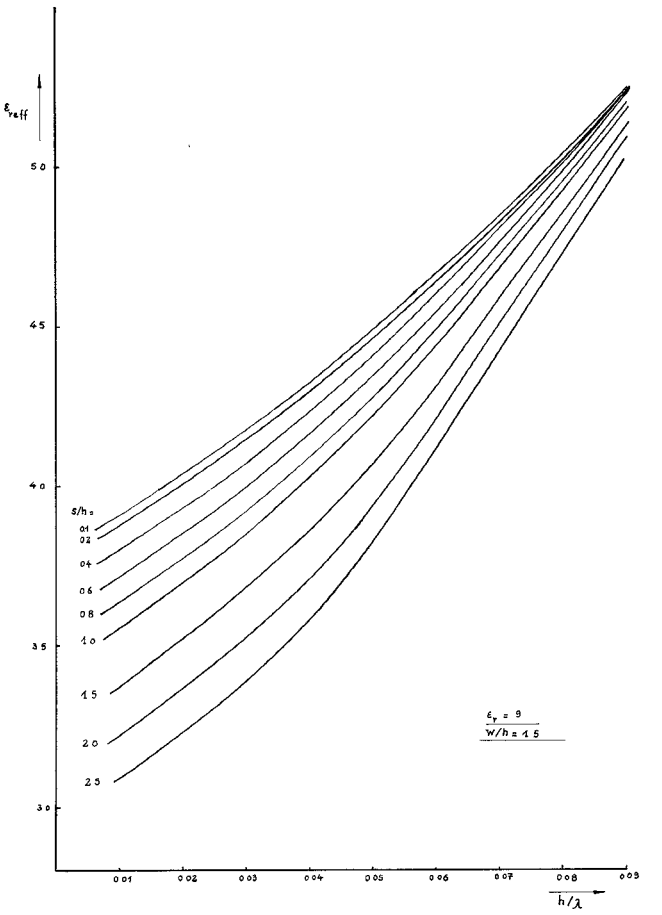

(a)

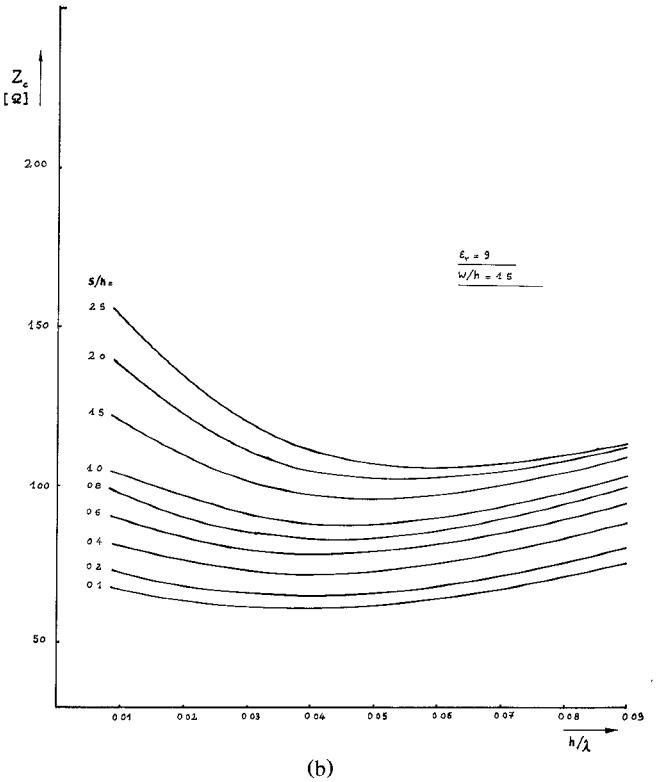

(b)

Fig. 2. (a) Dispersion characteristic of CPS's with s/h as parameter. $\epsilon_r = 9.0$, $w/h = 1.5$. (b) Characteristic impedance of CPS's with s/h as parameter. $\epsilon_r = 9.0$, $w/h = 1.5$.

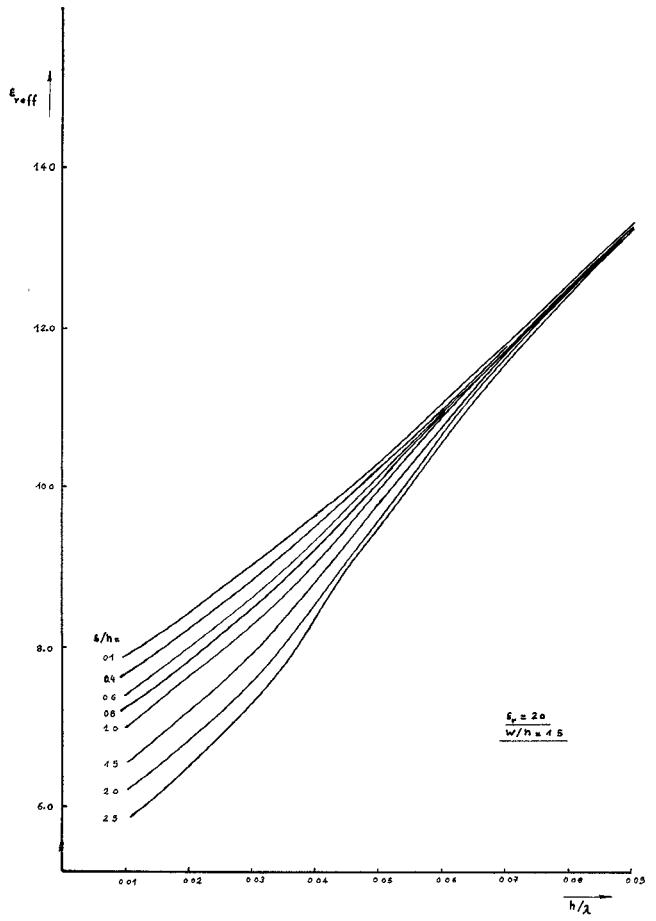

(a)

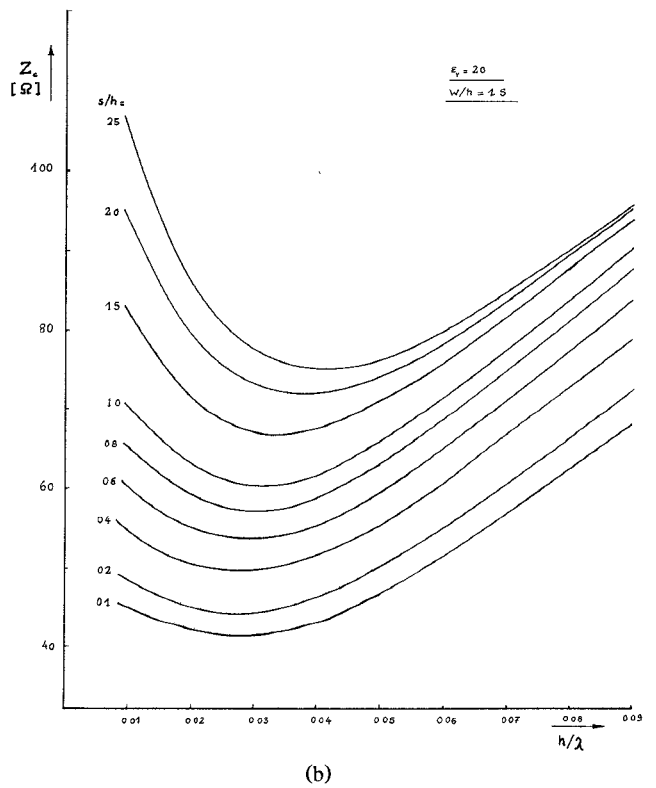

(b)

Fig. 3. (a) Dispersion characteristic of CPS's with s/h as parameter. $\epsilon_r = 20.0$, $w/h = 1.5$. (b) Characteristic impedance of CPS's with s/h as parameter. $\epsilon_r = 20.0$, $w/h = 1.5$.

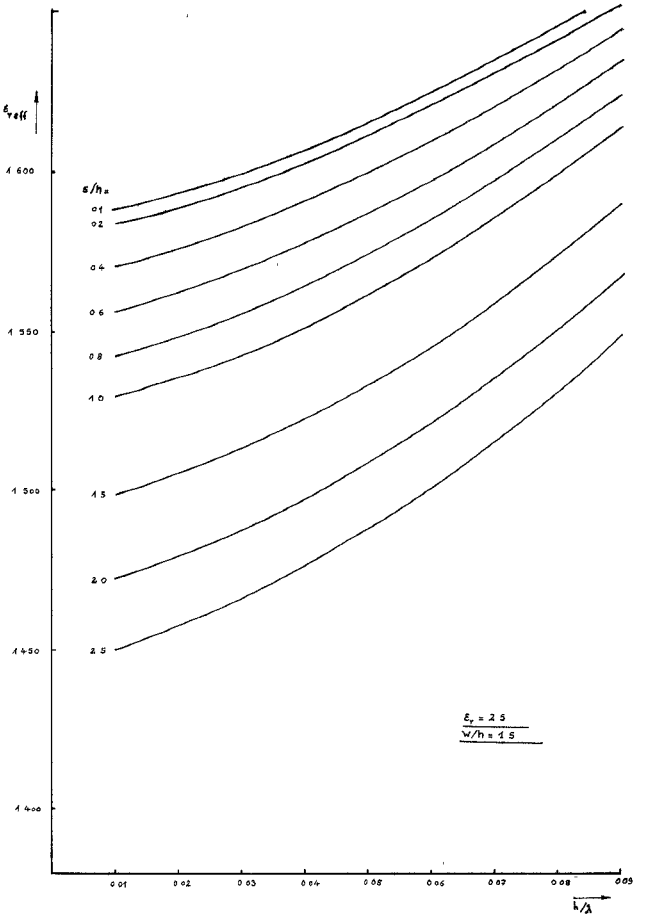

(a)

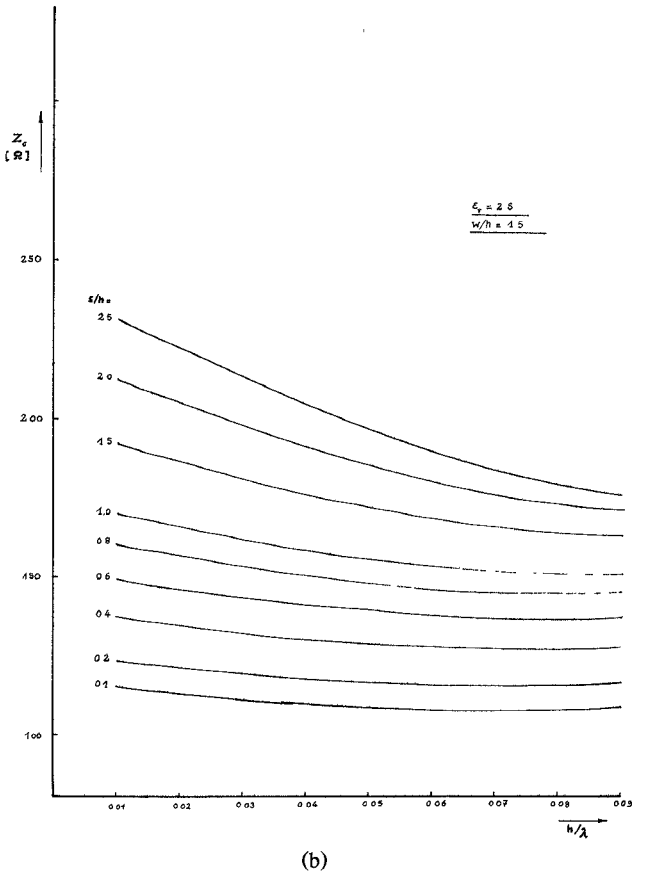

(b)

Fig. 4. Dispersion characteristic of CPS's with s/h as parameter. $\epsilon_r = 2.5$, $w/h = 1.5$. (b) Characteristic impedance of CPS's with s/h as parameter. $\epsilon_r = 2.5$, $w/h = 1.5$.

TABLE I
COMPARISON OF CALCULATED EFFECTIVE DIELECTRIC CONSTANT

h/λ	ereff [Present]			ereff [1]		
0.01	1.591	3.926	7.877	1.59	3.93	7.90
0.02	1.596	4.046	8.440	1.60	4.05	8.50
0.03	1.602	4.188	9.065	1.60	4.19	9.18
0.04	1.610	4.346	9.733	1.61	4.36	9.85
0.05	1.619	4.515	10.426	1.62	4.54	10.50
0.06	1.629	4.693	11.123	1.63	4.72	11.15
0.07	1.639	4.878	11.806	1.64	4.91	11.95
0.08	1.650	5.066	12.457	1.65	5.07	12.62
0.09	1.662	5.255	13.066	1.66	5.27	13.13
ϵ_r	2.5	9.0	20.0	2.5	9.0	20.0

$s/h = 0.1$; $w/h = 1.5$.

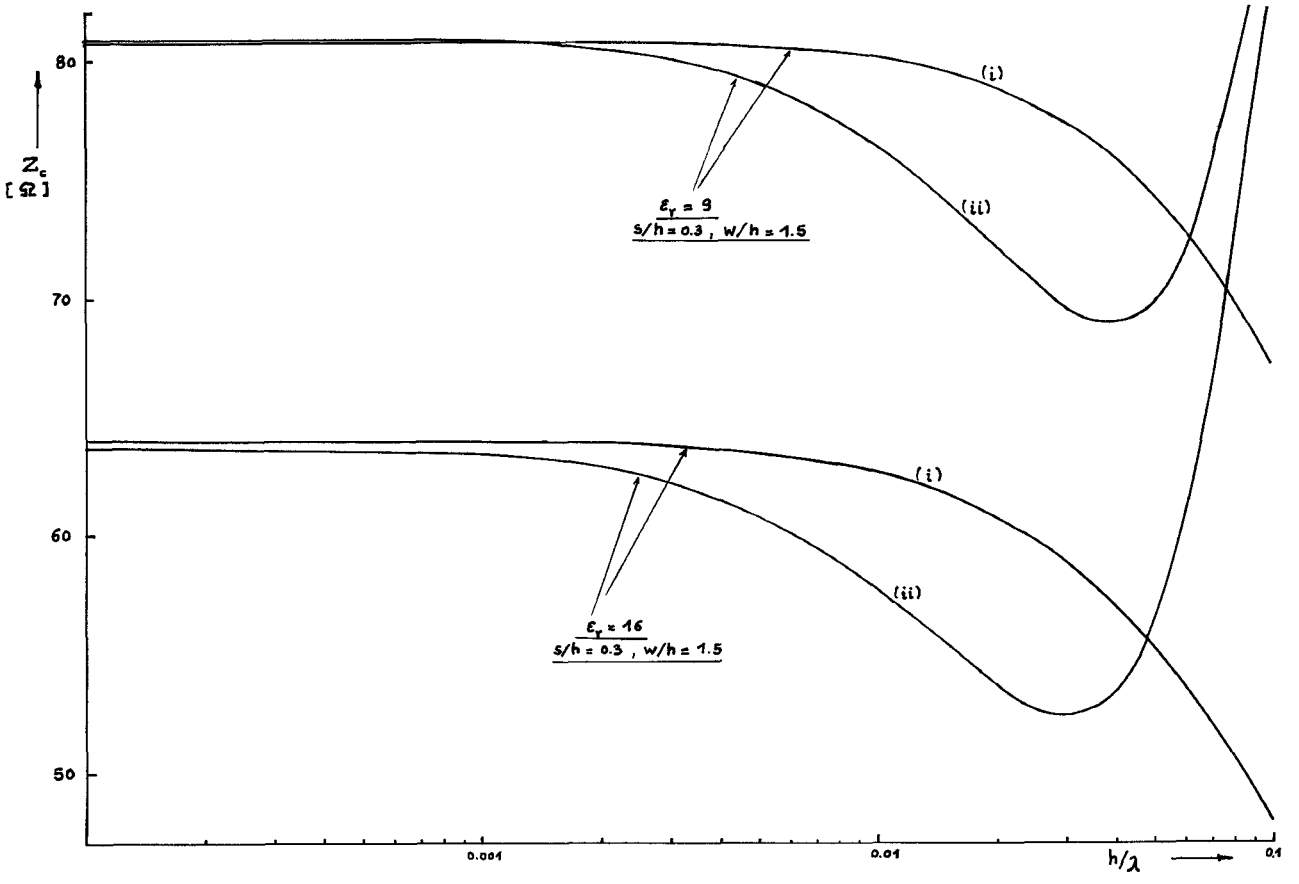

Fig. 5. Characteristic impedance according to different definitions.

versus the normalized frequency h/λ are shown in Figs. 2(a), 3(a), and 4(a). For comparison purposes, the material and geometric parameters have been chosen to be the same as in [1]. Allowing for the drawing tolerance, an excellent agreement between these dispersion characteristics and the corresponding results in [1] can be ascertained. This assessment is again documented in Table I, where typical results are shown.

Concerning the characteristic impedance, the same sets of material and geometric parameters have been used for its calculation according to definition (15). It may be mentioned here that the integrand in (17) as function of k_y has the same asymptotic behavior as the integrand of the stationary integral in (12). The numerical results are depicted in Figs. 2(b), 3(b), and 4(b). For the lower frequency region in these diagrams, there is only partially acceptable agreement with the results in [1], the present method yielding generally lower values. However, the important fact to notice here is that with increasing frequency the dispersive behavior of the impedance according to our results is fundamentally different from the behavior in [1], where a steady decrease is shown. In our case, in the upper frequency region there is a clear upward trend of the impedance with increasing frequency. Comparable behavior is encountered in the case of microstrip.

Fig. 5 shows the dynamic behavior of the characteristic impedance, on the base of the two different definitions, across an extended frequency range. Curves (*i*) pertain to the

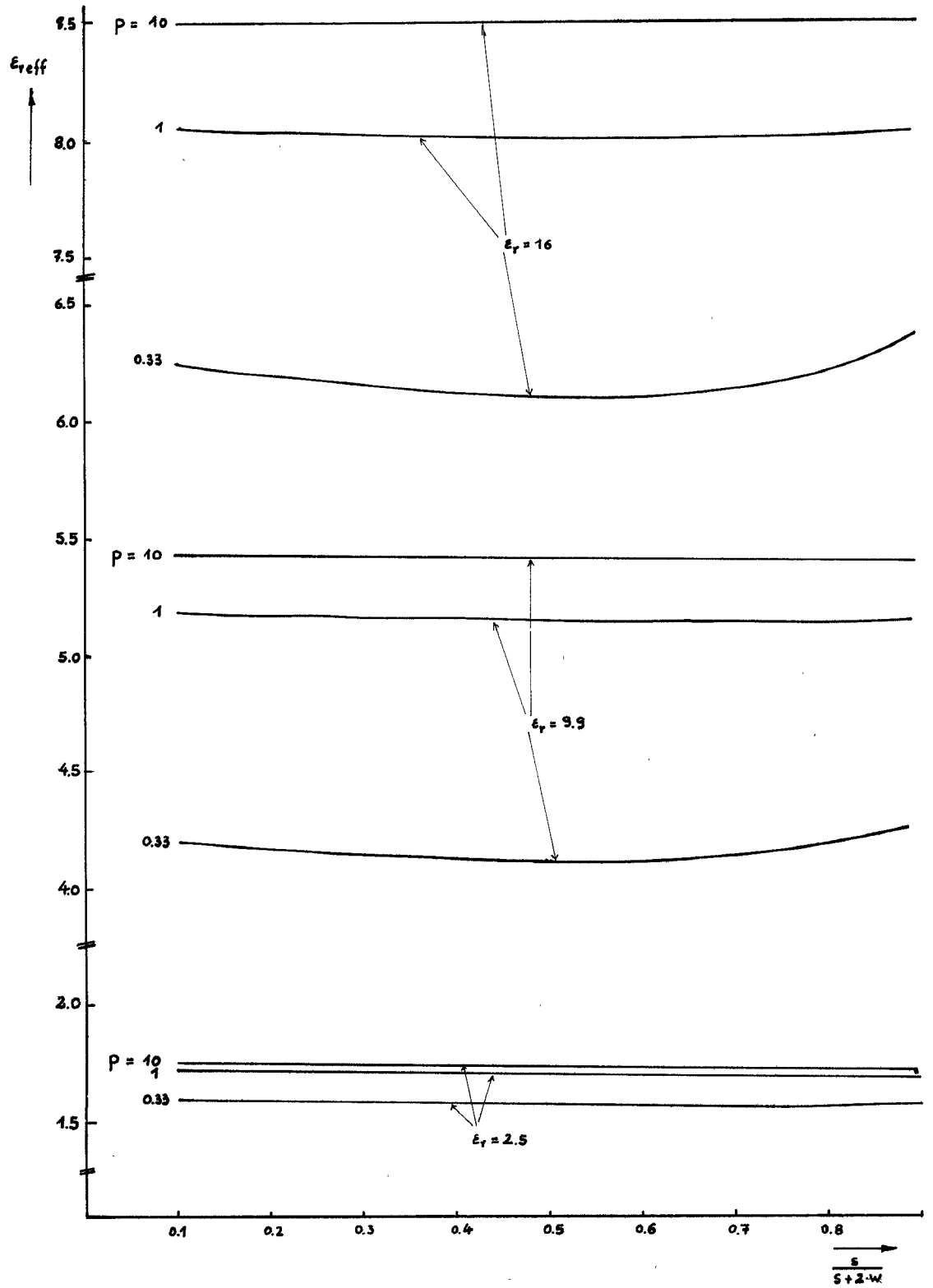

Fig. 6. ϵ_{reff} versus the geometric parameter (shape ratio) $s/(s+2w)$. The parameter p is defined as $p = h/(s+2w)$.

"ereff" definition in (13), curves (*ii*) to the transported-power related definition in (15). The expected convergence of the two definitions toward the same "static" value is confirmed. Toward the higher frequency region the line progressively departs from TEM-like propagation behavior; therefore the deviation between the two differently defined impedances is increasingly accentuated. It may be recalled here that the "ereff" definition is strictly valid for TEM configurations.

The diagrams of Fig. 6 demonstrate the influence of the geometry-dependent parameters on the propagation constant (in the practically dispersion-free lower frequency region). The ranges of parameter values for which practical

design applications are feasible can easily be determined from such diagrams.

VI. Conclusions

A spectral-domain stationary expression for the propagation constant ("ereff") and expressions for two different characteristic impedance definitions have been formulated for coplanar strips which allow an efficient and reliable analysis of this MIC transmission line. Numerical results have been presented which, with respect to the propagation constant, are in excellent agreement with results arrived at by means of an established, but nonetheless more expensive, method (Galerkin's method). Concerning the characteristic impedance, according to our results, there is a novel aspect of the dynamic behavior of this quantity. Contrary to previously published results showing a steady decrease of the impedance with increasing frequency, in our case the initial decrease was followed in the upper frequency region by an upward turn. The validity of different impedance definitions has been discussed on the base of representative numerical results.

Appendix I

The system of equations for the spectral amplitude coefficients has the form

$$[M][K]=[J]$$

with

$$[K]=\left[A_1^E, B_1^E, A_1^H, B_1^H, A_2^E, A_2^H, A_3^E, A_3^H\right]^T$$

$$[J]=\left[0,0,\tilde{J}_{sz},0,0,0,0,0\right]^T$$

and

$$[M]=\begin{bmatrix}
\delta^E\cosh(\gamma_1 h) & \delta^E\sinh(\gamma_1 h) & \gamma_1\sinh(\gamma_1 h) & \gamma_1\cosh(\gamma_1 h) & -\delta^E\epsilon_r & -\gamma_2 & 0 & 0\\
\cosh(\gamma_1 h) & \sinh(\gamma_1 h) & 0 & 0 & -e\cdot\epsilon_r & 0 & 0 & 0\\
\gamma_1\sinh(\gamma_1 h) & \gamma_1\cosh(\gamma_1 h) & -\delta^H\cosh(\gamma_1 h) & -\delta^H\sinh(\gamma_1 h) & \gamma_2 & \delta^H & 0 & 0\\
0 & 0 & \cosh(\gamma_1 h) & \sinh(\gamma_1 h) & 0 & -e & 0 & 0\\
\delta^E & 0 & 0 & \gamma_1 & 0 & 0 & -\epsilon_r\cdot\delta^E & -\gamma_2\\
1 & 0 & 0 & 0 & 0 & 0 & -e\cdot\epsilon_r & 0\\
0 & \gamma_1 & -\delta^H & 0 & 0 & 0 & -\gamma_2 & \delta^H\\
0 & 0 & 1 & 0 & 0 & 0 & 0 & -e
\end{bmatrix}$$

where

$$\delta^E=\frac{\beta\cdot k_y}{j\omega\epsilon_0\epsilon_r}\qquad \delta^H=\frac{\beta\cdot k_y}{j\omega\mu_0}\qquad e=\frac{1-\epsilon_{r\,\mathrm{eff}}}{\epsilon_r-\epsilon_{r\,\mathrm{eff}}}.$$

Appendix II

$$E_1=\epsilon_r^{-1}\left(1+e^{-2}(\gamma_2/\gamma_1)^2\right)+\gamma_1^{-2}\delta^E\cdot\delta^H(1-e^{-1})^2$$

$$E_2=1+e^{-2}(\gamma_2/\gamma_1)^2+\gamma_1^{-2}\cdot\delta^E\cdot\delta^H(1-e^{-1})^2$$

$$E_3=1+\epsilon_r^{-1}e^{-2}(\gamma_2/\gamma_1)^2+\gamma_1^{-2}\delta^E\cdot\delta^H(1-e^{-1})^2$$

$$\epsilon_1=2\cdot\epsilon_r^{-1}e^{-1}E_1^{-1}$$

$$\epsilon_2=2e^{-1}E_2^{-1}$$

$$\epsilon_3=2\epsilon_r^{-1}e^{-1}E_3^{-1}$$

$$\epsilon_4=E_1E_2^{-1}E_3^{-1}.$$

Acknowledgment

The author would like to thank Prof. Dr. R. Pregla, Hagen University, Germany, for helpful discussions during the preparation of this work.

References

[1] J. B. Knorr and K.-D. Kuchler, "Analysis of coupled slots and coplanar strips on dielectric substrate," *IEEE Trans. Microwave Theory Tech.*, vol. MTT-23, pp. 541–548, 1975.
[2] C. P. Wen, "Coplanar waveguide: A surface strip transmission line suitable for noncreciprocal gyromagnetic device application," *IEEE Trans. Microwave Theory Tech.*, vol. MTT-17, pp. 856–862, 1969.
[3] R. Pregla and S. G. Pintzos, "Determination of propagation constants in single and coupled microslots by a variational method," presented at 5th Colloquium on Microwave Communication, Budapest, 1974.
[4] R. F. Harrington, *Time-Harmonic Electromagnetic Fields*. New York: McGraw-Hill, 1961.
[5] W. Rumsey, "The reaction concept in electromagnetic theory," *Phys. Rev.*, vol. 94, pp. 1483–1491, 1954.
[6] S. G. Pintzos and R. Pregla, "A simple method for computing the resonant frequencies of microstrip ring resonators," *IEEE Trans. Microwave Theory Tech.*, vol. MTT-26, pp. 809–813, 1978.
[7] G. Kowalsky and R. Pregla, "Dispersion characteristics of single and coupled microstrips," *Arch. Elek. Übertragung.*, vol. 26, pp. 276–280, 1972.
[8] M. E. Hellman and I. Palocz, "The effect of neighboring conductors on the currents and fields in plane transmission lines," *IEEE Trans. Microwave Theory Tech.*, vol. MTT-17, pp. 254–259, 1969.
[9] R. K. Hoffmann, *Integrierte Mikrowellenschaltungen*. Berlin, Heidelberg, New York: Springer-Verlag, 1983.
[10] V. F. Hanna, "Finite boundary corrections to coplanar stripline analysis," *Electron. Lett.*, vol. 16, no. 15, pp. 604–606, 1980.
[11] G. Ghione and C. Naldi, "Analytical formulas for coplanar lines in hybrid and monolithic MIC's," *Electron. Lett.*, vol. 20, no. 4, pp. 179–181, 1984.

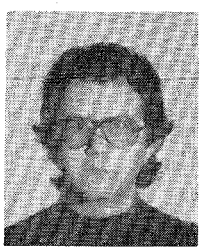

Sotirios G. Pintzos (M'74) was born on November 24, 1944, in Marcopoulo, Attika, Greece. He holds the Dipl.-Ing. degree in electrical engineering from the Technische Universitaet Braunschweig, Germany, and the Dr.-Ing. degree, also in electrical engineering, from Ruhr-Universitaet, Bochum, Germany.

From 1972 to 1978 he was with the Institut fuer Hoch- und Hoechstfrequenztechnik of the Ruhr-Universitaet Bochum as a Research Assistant. There he did research and taught in the area of applied electromagnetic theory and MIC applications. Since 1979 he has been with the Research Center of the Hellenic Navy (GETEN). His current interests are in the fields of microstrip antennas, computer-aided design for MIC and millimeter-wave components, and numerical methods in electromagnetics.

Dr. Pintzos is a member of VDE (ITG) and the Technical Chamber of Greece (TEE).